Beam Diagnostics and Applications

A. Hofmann

Chemin de l'Erse 20, CH-1218 Grand Saconnex, Switzerland

Abstract. Particle beams in accelerators are detected through the electromagnetic fields they create. Position and intensity monitors are based on the near field which stays attached to the charges. A large variety of measurements can be carried out with these devices. The closed orbit is obtained by reading out the position averaged over many turns. Change in the orbit resulting from a controlled deflection reveals the lattice functions. With a fast position monitor the betatron frequency can be measured. Its dependence on energy deviation, current, and quadrupole strength gives information on chromaticity, impedance, and local beta function. Turn-by-turn reading in all monitors allows one to check the optics and to measure the beta function and phase advance around the machine. Diagnostics based on the far field is done with synchrotron radiation. It is used to form an image of the beam cross section and to get its dimensions. Due to the small natural opening angle of the radiation, diffraction effects are important and limit the resolution. The angular spread of the particles in the beam can be measured by a direct observation of the emitted radiation.

ELECTROMAGNETIC FIELDS USED FOR BEAM DIAGNOSTICS

The beam diagnostics considered here are based on the electromagnetic fields created by the charged particles. We distinguish between the 'near field' and the 'far' or 'radiation field'. The near field is the Lorentz-transformed Coulomb field which now also contains a magnetic field. The electric field of a point charge on axis of a circular conducting chamber of radius a induces on the wall a charge distribution $q_w(s)$ having a rms width of $\sigma = a/\sqrt{2}\gamma$. Since this wall current pulse is very short for a relativistic particle, a bunch with longitudinal current distribution $I(t)$ induces on the wall a current $I_W(t)$ having practically the same form (see Figure 1). However, the wall current is of the opposite sign and does not contain the average beam current. The latter induces just a static charge which does not represent a current

$$I_w(t) \approx -(I(t) - \langle I \rangle).$$

Most beam position or intensity monitors are based on a measurement of the wall current. The loop or strip-line monitor shown in Figure 2 has a mixture of

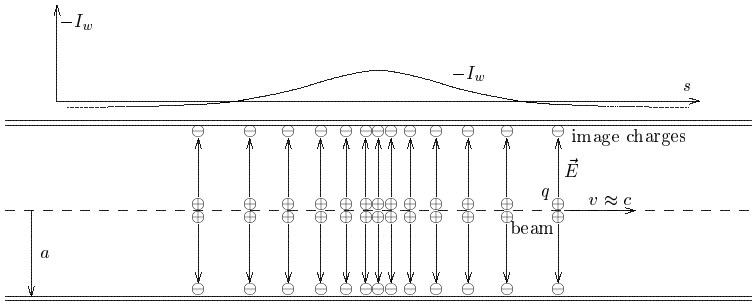

FIGURE 1. Wall current induced by a relativistic bunch.

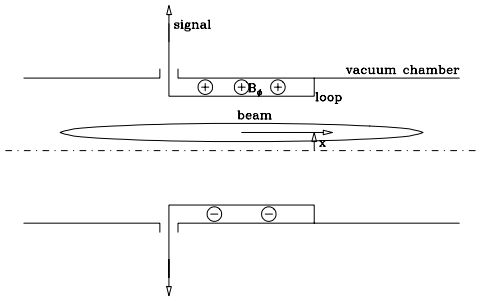

FIGURE 2. Loop monitor using, inductive and capacitive coupling.

inductive and capacitive coupling to the beam which depends on the width of the band forming the loop. The original wall current signal is generally distorted by the type of coupling used and the front end of the read-out system. Although the wall current induced by the beam does not contain the DC part, the latter can be estimated from the monitor reading between widely spaced bunches (see Figure 3) and determined directly from the average magnetic field produced by the beam outside the chamber.

Synchrotron light is the most common radiation field applied to beam diagnostics. It propagates through space and is not attached to the charges. In the majority of cases, it is used to form an image of the beam cross section to measure its dimensions. By observing the radiation directly we can determine its opening angle and measure the angular spread of the particles in the beam. Finally, from the time structure of the radiation we can determine the bunch length using a fast photon detector.

A position monitor uses the near-field which is attached to the beam and deter-

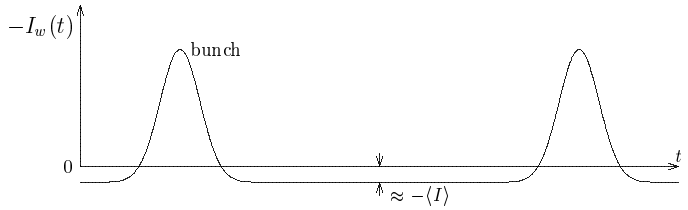

FIGURE 3. Monitor reading for widely spaced bunches.

mines the beam properties at the location of this monitor. However, monitors can also be sensitive to propagating radiation fields created far upstream in a bending magnet or in an aperture change close the monitor in form of diffraction radiation. Most monitors have a limited bandwidth lying below the cut-off frequency of the chamber and are therefore not sensitive to the propagating radiation fields.

MEASUREMENTS WITH BEAM POSITION MONITORS

We concentrate now on beam measurements which can be carried out with beam position monitors combined with deflectors. The accuracy and stability of position monitors have been greatly improved over the past years by precise and stable mechanical construction as well as by the use of state-of-the-art electronics. Furthermore alignment of the monitors with respect to the axis of the adjacent quadrupoles is now more precise. It is, in many machines, checked by moving the beam slowly in a quadrupole while observing the response to a strength modulation of this quadrupole. The observed position change due to the modulation is directly proportional to the distance of the beam from the quadrupole axis. The spatial difference between the electric center of the monitor and the magnetic axis of the quadrupole can be determined by this method and entered in the data analysis. This method, called often 'K-modulation', has been used in different laboratories [1]. With these improvements beam position measurements can reach an absolute accuracy of less than 0.1 mm and a resolution of a few microns. Many beam parameters can be determined by difference measurements where the beam position is obtained for two machine settings within a short time interval. The accuracy is in this case very high, since long-term drifts are avoided.

Position monitors can be used to give a turn-by-turn read out, allowing one to directly observe betatron oscillations and measure the tunes and their dependence on different parameters. At least one such monitor should be available in a storage ring. The demands in accuracy can be more relaxed then for the case of an orbit measurement. A bandwidth as large as the bunch frequency is desirable to check the filling pattern of the ring and to analyze coupled-bunch mode instabilities. Such a wide-band monitor can also observe phase oscillations directly without the need of dispersion. In the past, most machines had such monitors with a simple analog output displayed on a spectrum analyzer or a scope. In some proton machines a monitor of even larger bandwidth can be useful to measure the bunch length and to observe head-tail modes. For electron machines it is difficult to resolve the very short bunches. The corresponding measurements are usually carried out by detecting the synchrotron light with a fast device like a photodiode or a streak camera.

Some larger machines now have a possibility of turn-by-turn measurement in all position monitors to observe betatron oscillations and measure betatron phase advance and beta functions around the machine for optics checks.

The most important application of beam position monitors is the determination of the closed orbit around the ring followed by its correction with dedicated dipole magnets using special codes. We will not describe orbit corrections here but discuss a series of beam dynamics measurements which can be carried out with the help of the improved position monitors. Such experiments have been done in many machines. Here we select examples of a few rings for which the conditions and results were easily available.

AVERAGED READOUT TO MEASURE ORBIT

Measuring Optics from the Orbit Response to Local Deflections

We start with a system of monitors which measure the beam position averaged over many turns. This determines the closed orbit for stationary conditions by giving the horizontal and vertical coordinates

$$x_i = x_i(s_i) \ , \ \ y_i = y_i(s_i)$$

of all monitors i located at the longitudinal position s_i around the ring. As mentioned above, the most useful application of this information is the measurement of the closed orbit in a ring. From this, bending errors might be identified and corrected or the settings of the corrector magnets may be calculated, bringing the orbit as close as possible to the ideal.

We like to measure the effect of an applied deflection by a angle θ with a corrector magnet located at $s = 0$. Outside this deflector the orbit has the form of a betatron oscillation

$$x(s) = x(0)\sqrt{\frac{\beta(s)}{\beta(0)}}\cos(\phi(s) - \phi_0).$$

A local deflection by the angle θ imposes the condition

$$x(0) = x(2\pi R) \ , \ x'(0) - x'(2\pi R) = \theta.$$

Using the relation

$$\frac{d\phi}{ds} = \frac{1}{\beta}$$

we get for the orbit distortion created by a single deflection

$$x(s) = \frac{\theta}{2}\sqrt{\beta(s)\beta(0)}\frac{\cos(\pi Q - \phi(s))}{\sin(\pi Q)}.$$

In presenting this orbit distortion it is helpful to normalize the position monitor reading with $\sqrt{\beta}$ and display it against the betatron phase $\phi(s)$, as shown in Figure 4. The orbit has the form of a cosine with a cusp at the deflection error. This is, of course, only exact if the actual beta function agrees with the calculated one.

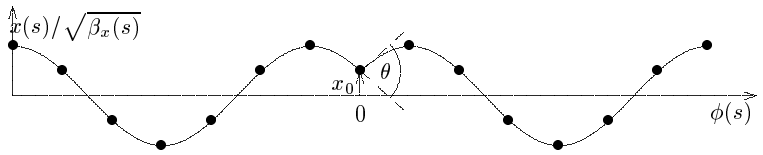

FIGURE 4. Orbit distortion caused by a single deflection.

A measurement of an orbit difference due to a known deflection θ determines the beta function. With a monitor at the location of the deflection magnet we measure a displacement $x_0 = x(0)$ given by

$$\beta(0) = \frac{2x_0 \tan(\pi Q)}{\theta}.$$

From this we obtain $\beta(0)$ if the tune Q is known. By measuring the position change at all monitors for sequential changes of all corrector magnets it is possible to determine the lattice functions around the ring. Since this problem is overdetermined also some checks of the monitor and corrector calibrations can be made. Such experiments have been successful to obtain the lattice function in storage rings with good accuracy [2].

Measuring Impedance from the Current Dependence of the Orbit

A circulating bunch induces a current in the chamber wall. This can lead to an energy loss if the beam surrounding has a resistive impedance. The loss per particle is proportional to the bunch current and is replaced by the rf cavities. For this reason a bunch has excessive energy when leaving the cavity and lacks energy entering the cavity after one turn. Beam position monitors located at finite dispersion D_x can measure this energy deviation from the relation $\Delta x = D_x \Delta p/p \approx D_x \Delta E/E$. By observing the orbit difference for two bunch currents, the resistive impedance distribution around the ring can be determined.

Such an experiment has been carried out in LEP [3] having two groups of cavities as shown left of Figure 5. The group in point 6 is powered while the other in point 2 is passive. The impedance of the latter and the one of the long arcs containing bellows, aperture changes, resistive walls, etc. can be determined separately. With a monitor in a dispersion-free region, it can be checked that there is no systematic current dependence of the monitor reading. The measured orbit difference for a change in bunch current is shown on the right of Figure 5. To increase accuracy, the readings of all monitors situated at the same dispersion value in one arc have been averaged. Since all arcs have the same properties, the obtained points are fitted with lines of the same slope. At point 2 there is a drop in orbit due to the

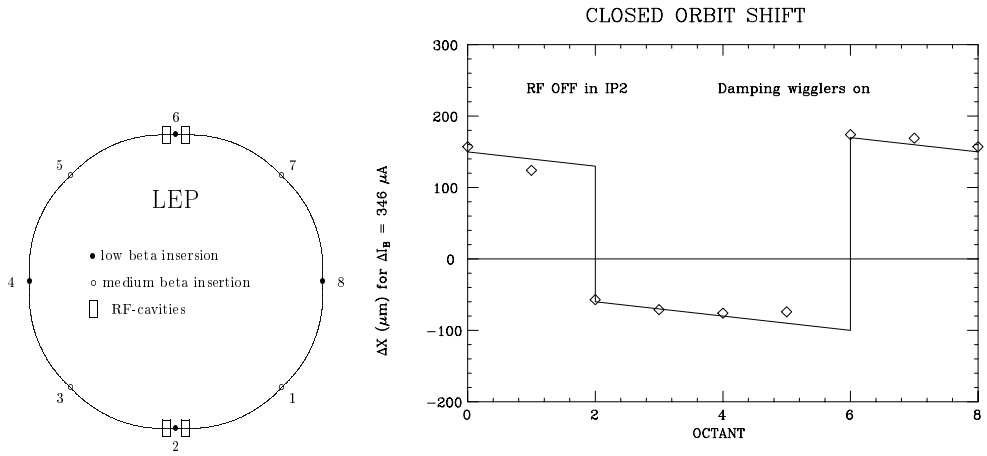

FIGURE 5. Difference orbit for two bunch currents in LEP having two rf sections. The cavities at point 6 are active, the ones at point 2 passive.

impedance of the cavities located there. The lost energy is replaced by the active cavities at point 6 and the orbit moves to the outside.

TURN-BY-TURN MEASUREMENTS IN ONE MONITOR

Observing Betatron Oscillations

A storage ring needs at least one monitor that can read the beam position turn by turn to observe betatron oscillations. This can also be achieved with an analog output of a bandwidth larger than the revolution frequency.

At the top of Figure 6 the readout of a position monitor at each turn k is shown for the observation of a betatron oscillation. Different harmonic fits can be made through the points. Since only one sample is taken at each revolution of the bunch, there is an ambiguity in the observed frequency ω_β which is related to the betatron tune Q by

$$\omega_\beta = \omega_0(n \pm Q).$$

The corresponding spectrum is shown at the bottom of the figure in units of the revolution frequency ω_0.

The most important application of this fast monitor is the measurement of the betatron tunes. To do this, we need a fast magnet which can produce a horizontal or vertical deflection within one revolution to excite betatron oscillations. This can be done either by giving the beam a relatively large kick and observing the free betatron oscillation or by a continuous harmonic excitation with a swept frequency. Noise-exciting and FFT spectrum analysis can also be used. The tune measurement

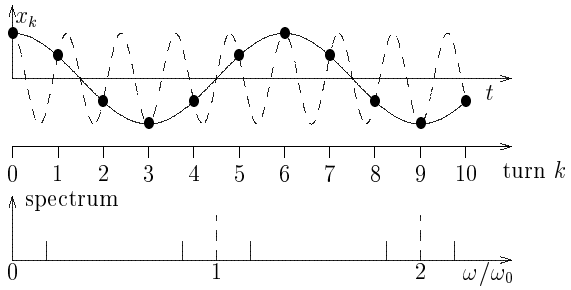

FIGURE 6. Betatron oscillation observed with a monitor having turn by turn read out.

is, in most machines, automated and can be used to study its dependence on different parameters:

- Measurement of the tune as a function of momentum $Q = Q(\Delta p/p)$ gives the chromaticity $Q' = dQ/(dp/p)$. The momentum, or energy, can be changed by a small variation of the rf frequency. This relation is given by the momentum compaction factor α_c and the Lorentz factor $\Delta p/p = -\eta \Delta f_{RF}/f_{RF}$ with $\eta = \alpha_c - 1/\gamma^2$.
- One of the fastest ways to obtain information about the impedance is a measurement of the tune as a function of bunch current $Q = Q(I_b)$. The field induced in the reactive transverse wall impedance by the bunch affects the focusing and therefore the tune.
- By measuring the tune as a function of oscillation amplitude $Q = Q(\hat{x})$ we obtain information about the non-linearity of the focusing. Increasing this amplitude until some beam loss occurs gives the acceptance of a ring, also called dynamic aperture.
- The beta function at a quadrupole can be measured by making a small variation ΔK of its strength parameter and observing the resulting change of the tune ΔQ. The short lens relation

$$\Delta Q = \frac{\beta \Delta K L}{4\pi}$$

directly gives the beta function. This is a very quick and important experiment to check the optics at some important locations, such as the low-beta insertion or the source point of synchrotron radiation. It is necessary that the quadrupoles involved have some independent powering. Some correction has to be made in the above relation for the finite length of the quadrupoles. In practice, the expected tune change for a given quadrupole variation is computed with an optics code and checked by the experiment. Hysteresis effects are important for small quadrupole strength variations. They can be checked with an integrator connected to an induction loop in the quadrupole which measures the actual field change.

- Coupling can be measured by kicking the beam in one plane and observing the oscillation in the other plane.
- If the bandwidth of the monitor is larger than the bunch frequency the filling pattern of the bunches can be checked. Furthermore, coupled bunch instabilities can be observed and the phase difference between the oscillation of individual bunches (coupled mode number), as well as the growth rate, can be determined. This information is often helpful to find the element driving the instability.

Beam Response — Transfer Function

The wide-band monitor combined with a deflection magnet can be used to measure the beam response to a pulse or a harmonic excitation. In addition to the observation of just the tune or the amplitude, we can measure the detailed response of the beam. In case of pulse excitation, this measurement contains a reading of the beam position at each turn after the kick. In the case of harmonic excitation we measure the amplitude and phase with respect to the driver, also called the beam transfer function. The time domain measurement is more popular with bunches while the transfer function is more suitable for continuous beams.

The beam transfer function measurement can be carried out with a network analyzer as indicated in Figure 7. For coasting (unbunched) beams, the theory and the measurement of the beam transfer function is particularly simple and therefore quite popular. In the transverse case the real (in-phase) part of the response gives directly the particle distribution in incoherent betatron frequency. An example of such a measurement in the ISR [4] is given in Figure 7. It shows that the phase changes by about π while sweeping through the betatron frequency distribution similar to the response of damped oscillator. In the longitudinal case one obtains the derivative of the energy distribution. Measuring the transfer function for different currents or distribution widths can give the complex impedance of the surroundings. A feedback system can be checked in phase and gain by taking the transfer function with and without it.

Experimental Tracking

The non-linear optics of a storage ring is often studied theoretically by particle tracking. A particle is launched with some initial offset and angle (x_0, x_0') and its trajectory calculated. After each revolution the coordinate pair (x_k, x_k') is plotted. In a linear machine these points are on an ellipse, however, non-linearities distort this curve. For some initial conditions particles get lost after some turns. By varying (x_0, x_0'), the dynamic acceptance can be determined.

We can study an existing machine experimentally with the same method. An angular deflection is given at some time and the beam position is observed turn by

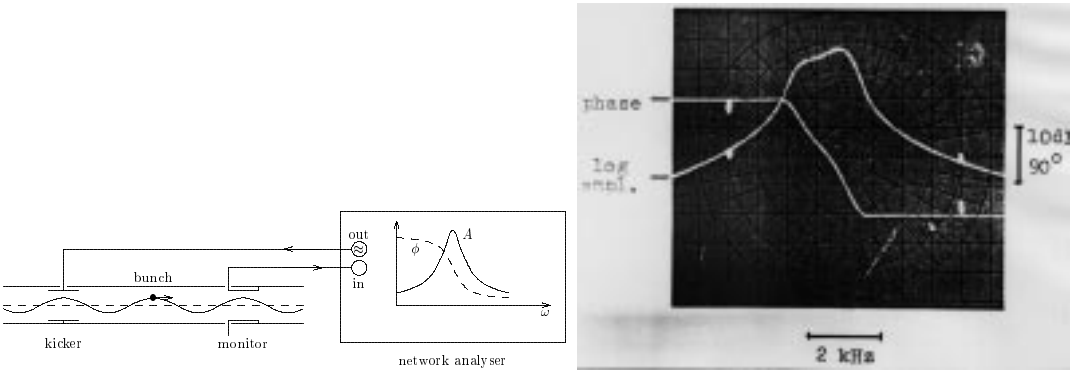

FIGURE 7. Transverse transfer function of a coasting beam.

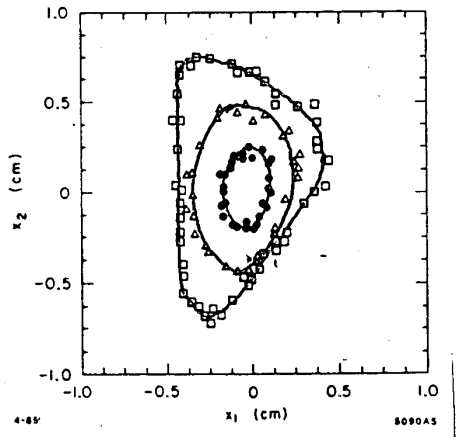

FIGURE 8. Experimental tracking in SPEAR.

turn, using two position monitors separated by a betatron phase of 90^0. These two monitors are equivalent to a measurement of position and angle at one location. In the case of electron beams, one probes the optics with different amplitudes due to the radiation damping. For protons the coherent signal disappears due to phase mixing but the amplitude of the individual particle stays constant. This makes the interpretation difficult. Usually one observes the beam for a limited number of turns and changes the initial kick to vary the amplitude. An example of such a measurement [5] with an electron beam in SPEAR is shown in Figure 8. An x, y-plot of the signals from the two monitors is made for a few turns at different amplitudes. The oscillation is quite linear at small amplitudes resulting in an ellipse on the plot. For larger amplitudes this figure has a triangular distortion due to the non-linearity and the proximity of the third-order resonance.

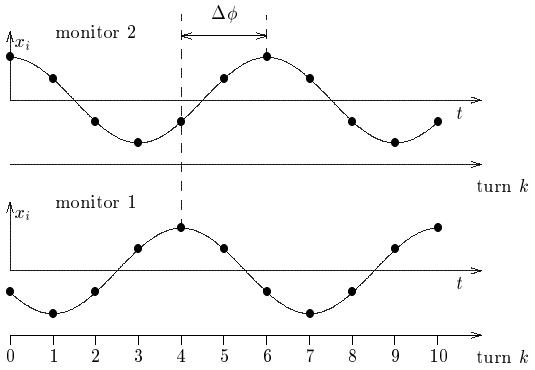

FIGURE 9. Betatron oscillation phase at two position monitors.

TURN-BY-TURN MEASUREMENTS IN ALL MONITORS

Measuring Phase Advance and Optics Checks

Turn-by-turn readout in all position monitors allows one to follow a betatron oscillation around the ring and measure the lattice functions. A betatron oscillation is excited and measured with many position monitors i around the ring every revolution k giving the readings

$$x_{ik} = \frac{\hat{x}}{\sqrt{\beta_{x0}}}\sqrt{\beta_{xi}}\cos(2\pi Q_x k + \mu_{xi}).$$

Comparing the phase of the oscillation observed in two monitors gives the betatron phase advance between them

$$\Delta\phi = \mu_{i+1} - \mu_i$$

as illustrated in Figure 9. The ratio of the beta functions is obtained from the square of the amplitude ratio observed between the two monitors.

$$\frac{\beta_{x,i+1}}{\beta_{x,i}} = \left(\frac{\hat{x}_{i+1,k}}{\hat{x}_{i,k}}\right)^2 .$$

The measurement of the phase advance has the advantage of having very small systematic errors. Once the signal is sufficiently clean to determine its phase it is unlikely to introduce errors in the form of delays. The measurement of the beta function ratio however depends on the monitor calibration. The relation between the optics functions

$$\Delta\phi = \mu_{i+1} - \mu_i = \int_{s_i}^{s_{i+1}} \frac{ds}{\beta(s)}$$

can be used to relate the two measurements.

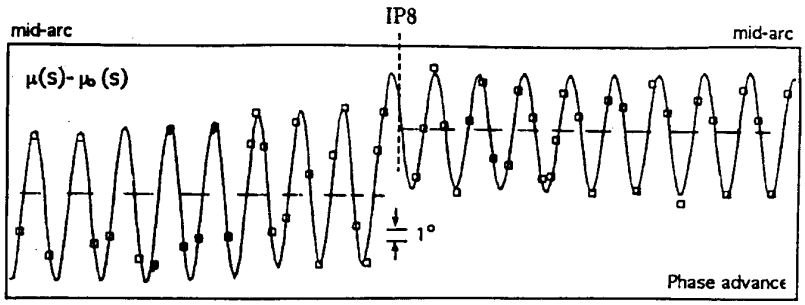

FIGURE 10. Beta beating caused by a focusing error.

By measuring the betatron phase around the ring and comparing it with the calculated one, we can check the beam optics and find errors. A local focusing deviation creates a beating of the beta function and the betatron phase advance around the ring. This deviation advances at twice the betatron wave number around the machine, that is, points being separated by $n\pi$ will keep this separation unless the error is located between them. An example of such a measurement in LEP [6] is shown in Figure 10. The difference between the measured and calculated betatron phase advance is plotted against the latter for about one eighth of LEP including a low-beta insertion at point 8. In the ideal case this plot should result in a straight line, however, due to a focusing error we observe a modulation of the line at twice the betatron phase advance with a phase jump at the interaction point IP8. Clearly an error is introduced by one or both strong quadrupoles of the low-beta insertion located around this point.

Measuring the Local Chromaticity and its Correction

The chromaticity gives the change of tune with momentum $Q' = dQ/(dp/p)$. In the absence of sextupole magnets, the chromaticity is negative since the focusing strength of the quadrupoles is smaller for particles with excess energy. With sextupole magnets located at finite dispersion this natural chromaticity can be corrected. To measure the chromaticity we make a small momentum change by varying the rf frequency and registering the difference in tune. Most rings operate with slightly positive chromaticity to stabilize head-tail modes. Strongly focusing sections, like low-beta insertions, produce negative chromaticity and are often at places of vanishing dispersion. The chromaticity cannot therefore be corrected locally but only at some distance. It might be interesting to study the local chromatic effects by measuring the phase advance as a function of momentum. Such an experiment was carried out in LEP [7] which has eight arcs with dispersion where the sextupoles are located and eight dispersion-free straight sections with low or medium beta insertions as shown on the left of Figure 11. The calculations and measurements of vertical chromatic phase advance $d\mu_y/(2\pi)/(dp/p)$ are shown on

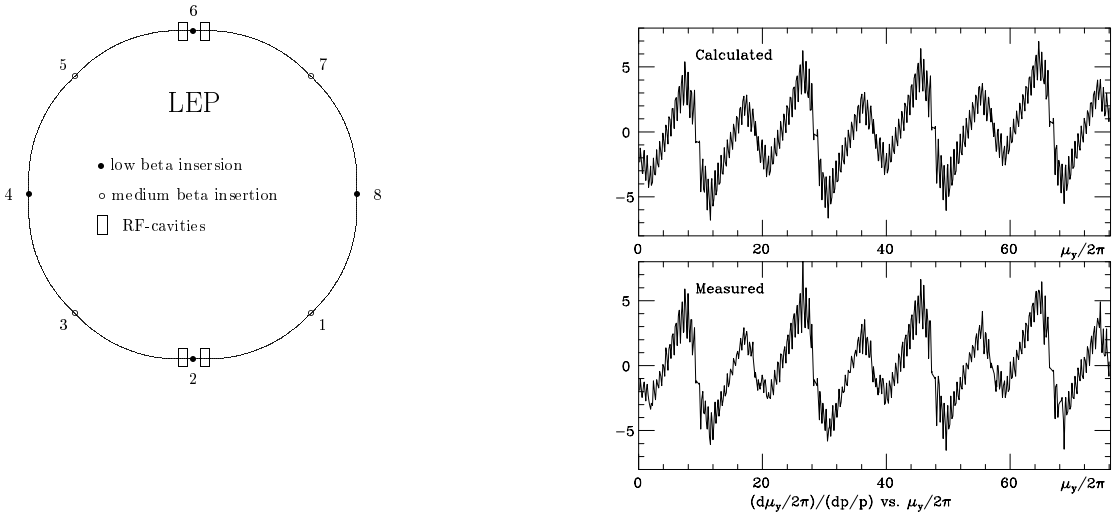

FIGURE 11. Calculation and measurement of the chromatic phase advance in LEP.

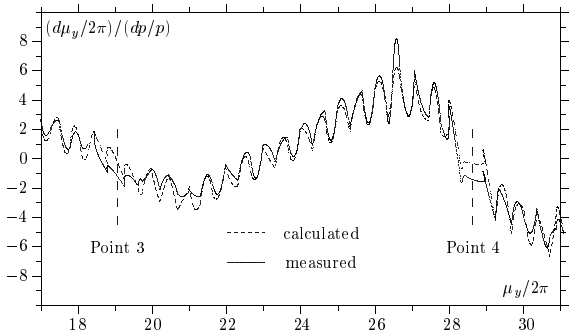

FIGURE 12. Detail of the chromatic phase advance showing a beta beating due to an optical mismatch of the off energy beam.

the right in Figure 11. Clearly visible are the negative slopes of this quantity in the four straight sections having strong focusing and the other four having medium focusing. In the arcs containing the sextupoles, this function has a compensating positive slope leading to a slightly positive chromatic phase advance around the whole ring. The agreement between calculation and measurement is very good and gives no indication of any error in the sextupole arrangement. There is a small modulation of this chromatic phase advance at twice the betatron wave number for both the calculated and the measured data shown in Figure 12 in more detail. This is due to the fact the chromatic effects are not corrected exactly where they occur. Particles with an energy deviation have therefore local focusing errors resulting in a modulation of the beta function which can only be corrected for some strategic places, like the interaction points.

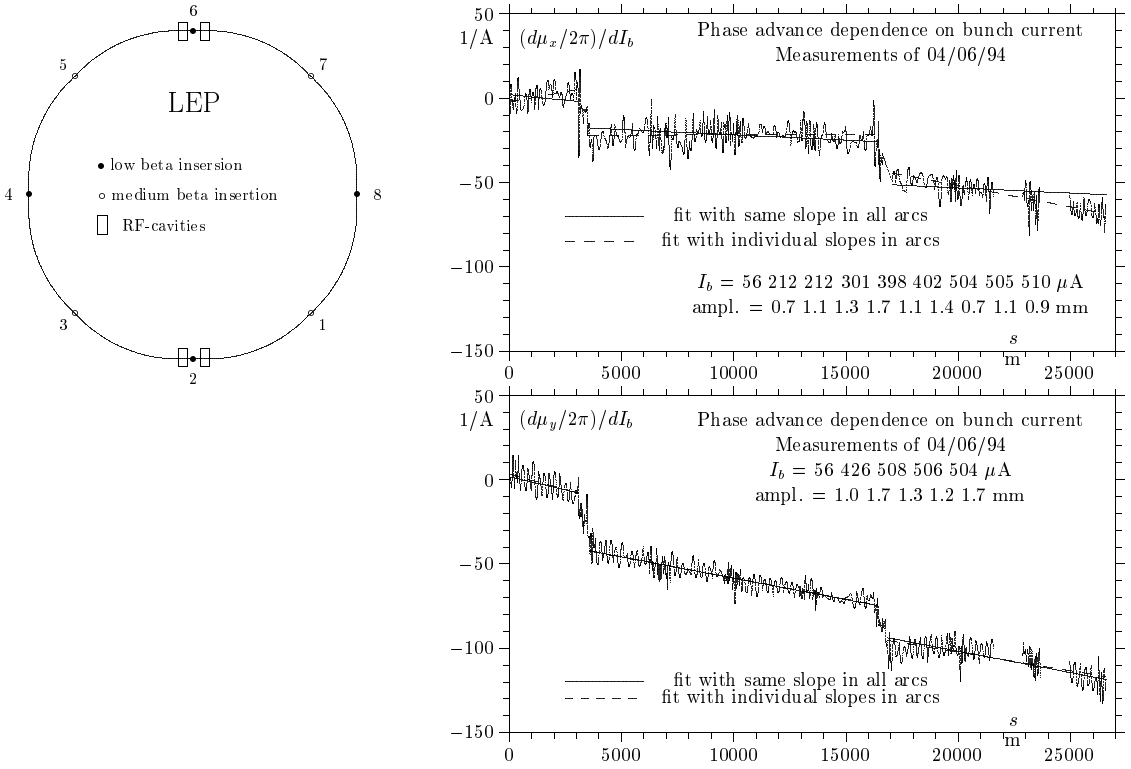

FIGURE 13. Horizontal and vertical phase advance vs. bunch current.

Phase Change with Current Due to the Transverse Reactive Impedance

The wall current induced by a circulating bunch, executing a betatron oscillation, produces fields through the transverse reactive impedance, which modify the focusing. This effect leads to a tune dependent on current and is often measured to estimate of the transverse impedance. By observing the betatron phase advance as a function of bunch current, we find the distribution of this impedance around the ring. In such an experiment [8] the betatron phase advance was measured for different currents in LEP which had at the time two groups of rf cavities as indicated on the left of Figure 13. The resulting dependence $d\mu/dI_b$ is plotted in the right part of this figure for both planes. It clearly shows a strong decrease of this quantity at the rf cavities and a more smooth change in the arcs. The cavities have a circular cross section and are expected to have the same transverse impedance in the horizontal and vertical plane. The arcs, however, have an elliptical chamber leading to an impedance being predominantly vertical. This expectation is clearly reproduced by the measurements which show no difference between the two planes at the cavities but have clearly a stronger slope in the arcs for the vertical plane.

DIAGNOSTICS WITH SYNCHROTRON RADIATION

Types of Measurements

Three main types of measurements are done with synchrotron radiation: imaging to measure the beam cross section, direct observation to measure the angular spread of the particles, and observing the longitudinal structure of the radiation to obtain the bunch length.

For the most common measurement, the radiation emitted tangentially in the bending magnet is extracted from the vacuum chamber through a window. A lens is then used to form an image of the source point on a screen, as illustrated in Figure 14.

It is also possible to observe the synchrotron radiation directly without using focusing elements, as shown in Figure 15. In this case one measures the angular distribution of the particles in the beam. If a long horizontal bending magnet serves as the source of the radiation, only the vertical angles can be measured. The resolution is limited by the natural opening angle of the radiation itself.

The bunch length can be measured by observing the time structure of the emitted radiation. Since the light pulse emitted by each individual particle is very short, the time distribution of the radiation directly reflects the longitudinal bunch shape. Such measurements depend on a fast photon detector and will not be discussed further here.

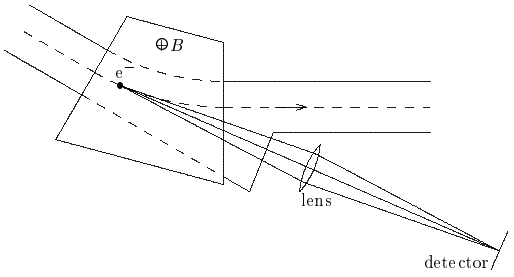

FIGURE 14. Imaging of the beam cross section with synchrotron radiation.

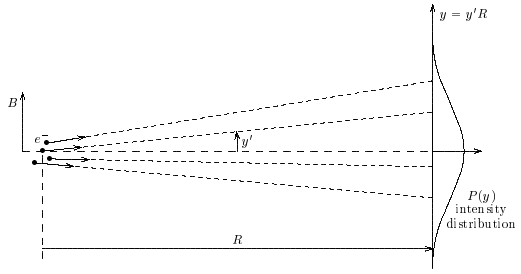

FIGURE 15. Direct observation of synchrotron radiation.

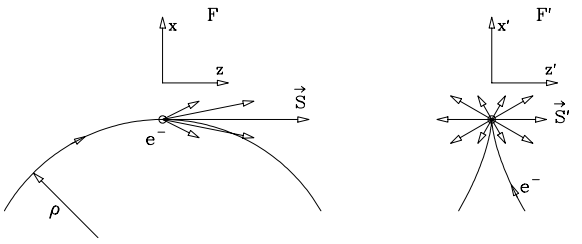

FIGURE 16. Opening angle of synchrotron radiation caused by the moving source.

Properties of Synchrotron Radiation

Many properties of synchrotron radiation can be understood from a qualitative treatment.

To estimate the opening angle we consider an electron moving in the laboratory frame F on a circular orbit and emitting synchrotron radiation (Figure 16). In an inertial frame F', which moves at one instant with the same velocity $\mathbf{v} = \boldsymbol{\beta} c$ as the electron, the particle trajectory has the form of a cycloid with a cusp where the electron undergoes acceleration in the $-x'$ direction. It will emit radiation which in this frame F' is approximately uniformly distributed. Going back to the laboratory frame F, by applying a Lorentz transformation, this radiation will be peaked forward. A photon emitted along the x'-axis in the moving frame F' will appear at an angle $1/\gamma$ in the laboratory frame F. The typical opening angle of synchrotron radiation is therefore of order $1/\gamma$ which is very small for ultra-relativistic particles where $\gamma \gg 1$.

The spectrum of synchrotron radiation depends on the type of magnet from which it originates. We consider first the usual case of a long magnet and estimate the typical frequency emitted by an electron and received by an observer P (Figure 17). The received radiation pulse is very short due to the small opening angle. The radiation seen first was emitted at point A, where the electron trajectory has an angle of $1/\gamma$ with respect to the direction towards the observer, and last at point A', where this angle is $-1/\gamma$. The length of the observed radiation pulse is the difference in travel time between electron and photon in going from A to A':

$$\Delta t = t_e - t_\gamma = \frac{2\rho}{\beta\gamma c} - \frac{2\rho \sin(1/\gamma)}{c} \approx \frac{2\rho}{\beta\gamma c}\left(1 - \beta + \frac{\beta}{6\gamma^2}\right) \approx \frac{4}{3}\frac{\rho}{c\gamma^3},$$

where we assumed the ultra-relativistic case $\gamma \gg 1$ and expanded the trigonometric function for small angles. The typical frequency is approximately

$$\omega_{typ} \sim \frac{2\pi}{\Delta t} \sim \frac{3\pi c\gamma^3}{2\rho}.$$

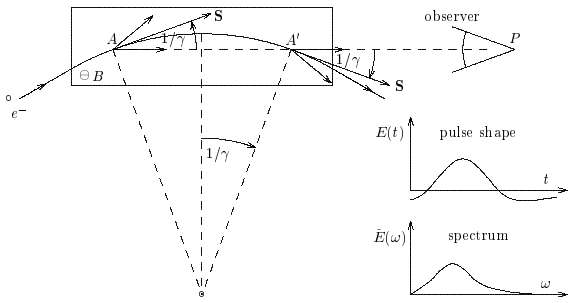

FIGURE 17. Spectrum of synchrotron radiation emitted in a long magnet.

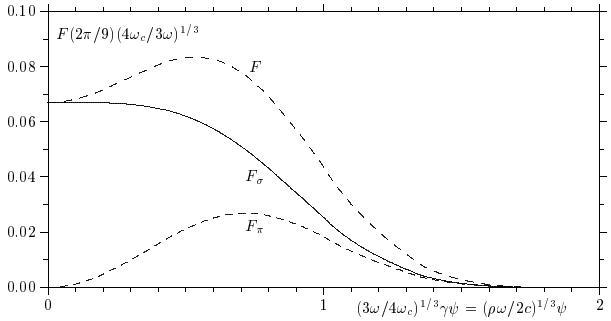

FIGURE 18. Vertical distribution of SR for $\omega \ll \omega_c$.

A quantitative treatment results in a critical frequency of similar magnitude

$$\omega_c = \frac{3c\gamma^3}{2\rho}$$

which divides the spectrum into two parts of equal power.

For diagnostics we like to use visible (or close to visible) light. This part of the spectrum is usually well below ω_c and approximations can be made. The calculated angular distribution for $\omega \ll \omega_c$ is shown in Figure 18 for the horizontal (σ-mode) and vertical (π-mode) polarization and for the total radiation. Here, it is independent of γ. The vertical rms opening angle for the σ-mode is

$$\sqrt{\langle \psi_\sigma^2 \rangle} \approx 0.41\,(\lambda/\rho)^{1/3}\,.$$

An undulator is an interesting source of synchrotron radiation. It consists of a spatially periodic magnetic field with period length λ_u in which the particle moves on a sinusoidal orbit (Figure 19). Each of the periods represents a source of radiation. These contributions emitted towards an observer at an angle θ will interfere with each other. We get maximum intensity at a wavelength λ for which the contributions from different undulator periods are in phase. The time difference ΔT between the arrival of adjacent contributions is in ultra-relativistic approximation

$$\Delta T = \frac{\lambda_u}{\beta c} - \frac{\lambda_u \cos\theta}{c} = \frac{\lambda_u(1-\beta\cos\theta)}{\beta c} \approx \frac{\lambda_u}{\beta c}\left(1-\beta+\frac{\theta^2}{2}\right) \approx \frac{\lambda_u}{2c\gamma^2}(1+\gamma^2\theta^2).$$

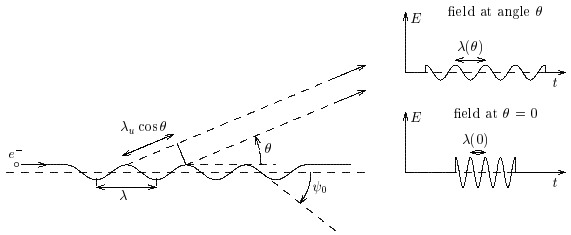

FIGURE 19. Spectrum of synchrotron radiation emitted in an undulator.

The frequency for which we get constructive interference is just $\omega = 2\pi/\Delta T$:

$$\omega = \frac{4\pi c\gamma^2}{\lambda_u(1+\gamma^2\theta^2)}.$$

Harmonics of this frequency might also be emitted.

Since for undulator radiation both the horizontal and vertical opening angles are small, direct observation gives the angular spread of the particles in both planes.

Imaging with Synchrotron Radiation

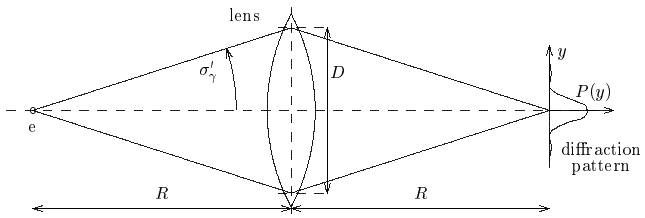

FIGURE 20. Imaging the beam cross section with synchrotron radiation.

We use synchrotron radiation to form a 1:1 image of the beam cross section with a single lens (Figure 20). Due to the small vertical opening angle of $\psi \approx 1/\gamma$ only the central part of the lens is illuminated. Similar to optical imaging with limited lens aperture D, this leads to a diffraction limit in the resolution d (half image size):

$$d \approx \frac{\lambda}{2D/R}.$$

For horizontally polarized synchrotron radiation from long magnets we found an rms opening angle $\sigma'_\gamma = \psi_{\sigma-rms} \approx 0.41(\lambda/\rho)^{1/3}$. Taking $D \approx 4\sigma_\gamma R$ we get $d \approx 0.3(\lambda^2\rho)^{1/3}$. A more quantitative treatment using Fraunhofer diffraction gives an rms image size

$$\sigma_y = 0.21(\lambda^2\rho)^{1/3}.$$

The resolution improves with small λ and ρ and is limited in large machines.

Measurement Examples

Imaging with Synchrotron Radiation in LEP

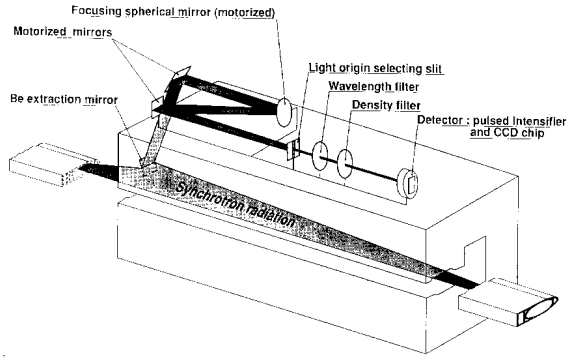

FIGURE 21. Telescope for imaging in LEP.

In LEP ($\rho = 3096$ m) a telescope ($\lambda \geq 200$ nm) is used (Figure 21) to image the beam [9]. Fraunhofer diffraction gives a vertical resolution of $\sigma_y \approx 0.1$ mm which is comparable to the beam size at E=45 GeV. Using a CCD camera and image processing, 3D plots, projections, and turn-by-turn reading are obtained.

Imaging with X-Ray Pin-Hole Camera

Since the resolution is $\propto (\lambda^2 \rho)^{1/3}$ the use of x-rays gives better results but optics elements are more difficult to implement. A simple pin-hole was used at CEA, [10]. The radiation originates in magnet with $\rho = 26.2$ m, reaches a pin-hole of 0.07 mm diameter after 8 m, and is detected 16 m further on a film (Figure 22). Absorption in 1.3 mm of Al and 6 m of air and film sensitivity gives $\lambda \approx 0.05$ nm as the dominant wave length. Diffraction effects are small but pin-hole size and film give a resolution of about 0.1 mm. It was used to minimize coupling by powering some quadrupoles to separate the tunes.

Direct Observation of Undulator Radiation in PEP

The radiation from an undulator in PEP was observed directly to get the horizontal and vertical angular spread of the electrons [11]. The emitted radiation passes through a monochromator to a screen (Figure 23). The undulator spectrum is measured and the beam picture on the screen observed. The one taken close to the undulator peak is scanned and corrected for the known natural distribution of the undulator radiation, the instrument resolution, and the beam size due to energy spread and dispersion at the source. With the known value of the electron beam lattice function at the source, the emittance of the electron beam is obtained.

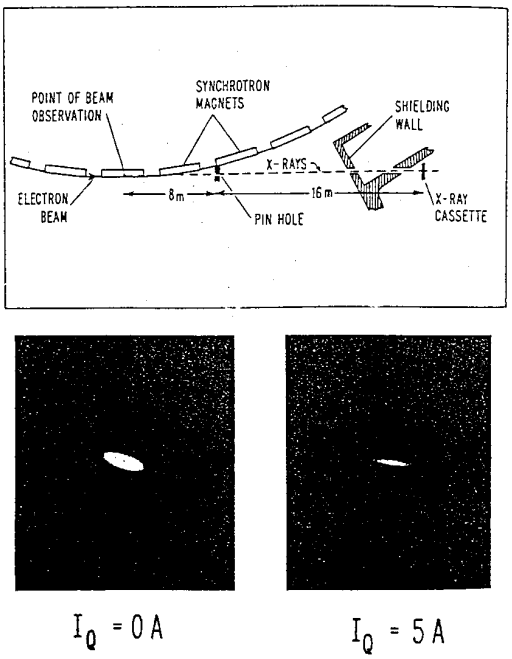

FIGURE 22. Imaging with an x-ray pin-hole camera.

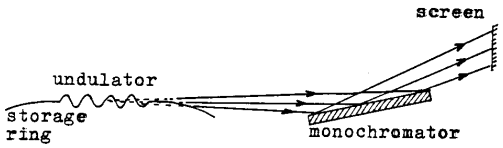

FIGURE 23. Direct observation of monochromatized x-rays in PEP.

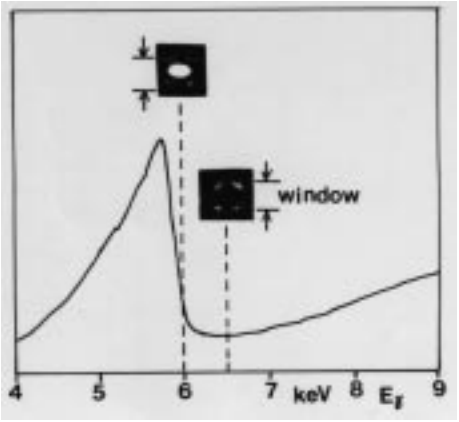

FIGURE 24. Measured undulator spectrum and photon beam picture.

REFERENCES

1. Tecker, F., B. Dehning, P. Galbraith, K. Hendrichsen, M. Placidi, and R. Schmidt, "Beam Position Monitor Offset Determination at LEP," Proceedings of the 1997 Particle Accelerator Conference, Vancouver (1997).
2. Robin, D., G. Portmann, H. Nishimura, and J. Safranek; "Model Calibration and Symmetry Restoration of the Advanced Light Source," in *Proceedings of EPAC96* (conference held in Sitges (Barcelona)), pp. 971–973 (1996).
3. Brandt, D., P. Castro, K. Cornelis, A. Hofmann, G. Morpurgo, G. L. Sabbi, J. Wenninger, and B. Zotter; "Measurement of Impedance Distributions and Instability Thresholds in LEP," in *Proceedings of the 1995 Particle Accelerator Conference* (conference held in Dallas), pp. 570–572 (1995).
4. Hofmann, A. and B. Zotter, "Measurement of Beam Stability and Coupling Impedance by RF Excitation," in *Proc. of the 1977 Particle Accelerator Conference*, IEEE Trans. on Nucl. Sci. NS 24-3, pp. 1487–1489 (1977).
5. Morton, P. L., J. L. Pellegrin, T. Raubenheimer, L. Rivkin, M. Ross, R. D. Ruth, W. L. Spence; "A Diagnostic for Dynamic Aperture," in *Proceedings of the 1995 Particle Accelerator Conference*, IEEE Trans. on Nucl. Sci., NS-32-5, pp. 2291–2293 (1985).
6. Borer, J., C. Bovet, A. Burns, and G. Morpurgo; "Harmonic Analysis of Coherent Bunch Oscillations in LEP," in *Proceedings of EPAC92* (conference held in Berlin), pp. 1082–1084 (1992).
7. Brandt, D., P. Castro, K. Cornelis, A. Hofmann, G. Morpurgo, G. L. Sabbi, and A. Verdier; "Measurement of Chromatic Effects in LEP," in *Proceedings of the 1995 Particle Accelerator Conference* (conference held in Dallas, 1995).
8. Brandt, D., P. Castro, K. Cornelis, A. Hofmann, G. Morpurgo, G. L. Sabbi, J. Wenninger, B. Zotter; "Measurement of Impedance Distributions and Instability Thresholds in LEP," in *Proceedings of the 1995 Particle Accelerator Conference*, Dallas (1995).
9. Bovet, C., G. Burtin, R. J. Colchester, B. Halvarsson, R. Jung, S. Levitt, and J. M. Vouillot, "The LEP Synchrotron Light Monitors," CERN SL/91-25 and *Proceedings of the 1991 IEEE Particle Accelerator Conference*, p. 1160.
10. Hofmann, A., and K. W. Robinson, "Measurement of the Cross Section of a High-Energy Electron Beam by means Portion of the Synchrotron Radiation", in *Proceedings 1971 Particle Accelerator Conference, IEEE Trans. Nucl. Sci.* NS 18-3, p. 973 (1971)
11. Brendt, M., G. Brown, R. Brown, J. Cerino, J. Christensen, M. Donald, B. Graham, R. Gray, El Guerra, C. Harris, A. Hofmann, C. Hollosi, T. Jones, J. Jowett, R. Liu, P. Morton, J. M. Paterson, R. Pennacchi, L. Rivkin, T. Taylor, T. Troxel, F. Turner, J. Turner, P. Wang, H. Wiedemann, and H. Winick, "Operation of PEP in a Low Emittance Mode," in *Proceedings of the 1987 IEEE Particle Accelerator Conference*, p. 461 (1987).